Magnetic-ion-pair interaction in (Cd,Mn)Te and (Cd,Mn)Se using spin-flip Raman scattering and magnetization

E. D. Isaacs,* D. Heiman, and P. Becla
Francis Bitter National Magnet Laboratory, Massachusetts Institute of Technology, Cambridge, Massachusetts 02139

Y. Shapira
Department of Physics, Tufts University, Medford, Massachusetts 02155
and Francis Bitter National Magnet Laboratory, Massachusetts Institute of Technology, Cambridge, Massachusetts 02139

R. Kershaw, K. Dwight, and A. Wold
Department of Chemistry, Brown University, Providence, Rhode Island 02912
(Received 9 May 1988)

Isolated Mn ion pairs in dilute magnetic semiconductors exhibit steplike increases in the total spin alignment with increasing magnetic field. These steps in $Cd_{1-x}Mn_xTe$ and $Cd_{1-x}Mn_xSe$, with $x \leq 0.05$, are studied using spin-flip Raman scattering and magnetization measurements at $0.5 \leq T \leq 1.3$ K. In dc fields to 30 T the optical spectra show three steps for (Cd,Mn)Te and two for (Cd,Mn)Se. Analysis of the field positions of the steps obtained by both methods gives the nearest-neighbor exchange constant $J_{NN}/k_B = -6.1 \pm 0.2$ K for the telluride and -7.7 ± 0.3 K for the selenide. By comparison of the optical and magnetization results, the *s-d* exchange parameter for (Cd,Mn)Te is found to be $\alpha N_0 = 211 \pm 10$ meV.

I. INTRODUCTION

High-field magnetization steps in dilute magnetic semiconductors (DMS) with low magnetic ion concentrations ($x < 0.1$) have recently been the subject of many investigations.[1-12] The steps arise from field-induced energy-level crossings of nearest-neighbor (NN) pairs of antiferromagnetically coupled spins. For a pair of Mn^{++} ions (each with spin $S = \frac{5}{2}$) there are five magnetization steps corresponding to transitions between levels with total spin $S_T = 0, 1, \ldots, 5$. Analysis of the first few steps gives a value for the NN exchange constant J_{NN} and has shown that the ions are distributed randomly over the cation sites.

Previous studies of magnetization steps have employed the techniques of direct magnetization,[1-3,7,9-11] reflectivity,[4-6] photoluminescence,[8] magnetoresistance,[7] and Faraday rotation.[12] Results have been reported for (Cd,Mn)Se, (Cd,Mn)S, (Cd,Mn)Te, (Zn,Mn)Se, (Zn,Mn)Te, and (Hg,Mn)Te. Here, we present the first studies of magnetization steps using the technique of spin-flip Raman scattering (SFRS) from electrons. The experiments were carried out on (Cd,Mn)Se and (Cd,Mn)Te in dc fields up to 30 T. For (Cd,Mn)Se we observe two full steps, whereas previous studies only partially revealed the second step.[2] For (Cd,Mn)Te part of the third step is observed for the first time—the first two steps were previously measured by direct magnetization,[11] and by reflectivity.[5]

SFRS is a new, valuable tool for determining J_{NN}. The Stokes shift, which is related to the magnetization, can be measured with a sufficient accuracy to reveal the steps clearly. An important advantage of the SFRS method is that with the new fiber-optic apparatus[13] it can be used in the hybrid magnet (superconductor + Bitter solenoids) which produces dc fields up to 30 T. (Other techniques in dc fields are presently operational only below 23 T.) To assess the merits of the new SFRS technique, the SFRS measurements were supplemented by direct magnetization measurements on the same materials. Here, a new magnetometer (superior to those used earlier in high-field work) was used. This resulted in a substantial improvement over older magnetization data[1] for (Cd,Mn)Se. By combining the SFRS and magnetization data we also determine the *s-d* exchange parameter (αN_0) for (Cd,Mn)Te.

II. THEORETICAL BACKGROUND

A. Average spin alignment and cluster model

When a magnetic field B is applied along the z axis, the Mn^{2+} ions acquire a nonzero average spin component $\langle S_z \rangle$ per ion. The magnetization per gram is related to $\langle S_z \rangle$ by

$$M(B) = \left[\frac{2\mu_B x A}{W} \right] | \langle S_z \rangle | \ , \tag{1}$$

where μ_B is the Bohr magneton, A is Avogardo's number, and W the gram molecular weight. Here, it was assumed that the g factor for the Mn^{2+} ions is $g = 2.0$, in close agreement with available data.[3,11]

In DMS with low x values, $\langle S_z \rangle$ is well approximated by a sum of contributions due to isolated clusters of

spins.[1,14,15] If we ignore all exchange interactions except those between nearest-neighbors (NN cluster model), then for $x \leq 0.05$ it is sufficient to consider only four types of clusters: (1) isolated Mn^{2+} spins, (2) isolated pairs of NN spins, (3) open triangles, and (4) closed triangles of NN spins. For $x=0.05$, 54% of the spins are singles, 24% in pairs, 11% in triplets (triangles), and the remaining 11% in larger clusters. The NN cluster model is a useful first approximation for describing the magnetization at high fields and low T because interactions between next-nearest neighbors (NNN) and more distant neighbors only become important in low magnetic fields and at low temperatures.[16]

B. Magnetization steps

All clusters other than single-isolated spins give rise to magnetization steps at high fields and low T.[1] However, in DMS which contain Mn^{2+} ions the only steps which are readily observed below 30 T arise from isolated pairs of NN spins. The magnetic field positions of these steps, *assuming NN interactions only,* can be determined from the Hamiltonian for an isolated pair of NN ions with spins $\mathbf{S}_1$ and $\mathbf{S}_2$,

$$\mathcal{H}_{\text{pair}} = -2J_{\text{NN}}\mathbf{S}_1\cdot\mathbf{S}_2 + g\mu_B(S_{1z}+S_{2z})B_z \ . \tag{2}$$

The energy eigenvalues are

$$E_{\text{pair}} = [-J_{\text{NN}}S_T(S_T+1) - \tfrac{35}{2}] + g\mu_B mB \ , \tag{3}$$

with $S_T = 0, 1, \ldots, 5$, and $m = S_T, S_T-1, \ldots, -S_T$. For small magnetic fields the ground state of the pair has $S_T = m = 0$. At the magnetic field B_1, defined by

$$g\mu_B B_1 = 2\,|\,J_{\text{NN}}\,| \ , \tag{4}$$

the ground state becomes $S_T = 1, m = -1$ and the first step occurs. The other steps occur at $g\mu_B B_n = 2n\,|\,J_{\text{NN}}\,|$, where n is a positive integer ≤ 5.

At low temperatures ($k_B T \ll |\,J_{\text{NN}}\,|$) and for $x \leq 0.05$ the average moment per magnetic ion is principally the sum of two contributions: (1) a part that saturates at low magnetic fields ($B < 10$ T), which is mostly due to the isolated spins, plus (2) a part due to the magnetization steps of the pairs. The total $\langle S_z \rangle$ can then be written as

$$|\langle S_z\rangle| = \frac{5}{2}\left[\frac{\bar{x}}{x}\right]\mathcal{B}_{5/2}(y) + \tfrac{1}{2}P_2 \sum_n \left[1+\exp\left[\frac{g\mu_B}{k_B T_{\text{eff}}}(B_n - B)\right]\right]^{-1} . \tag{5}$$

The first term contains the Brillouin function $\mathcal{B}_{5/2}(y)$ where $y = 5\mu_B B/k_B(T+T_0)$, $\bar{x}$ is the *effective* molar concentration, T_0 is a phenomenological temperature describing more distant neighbor interactions,

$$P_2 = 12x(1-x)^{18} \tag{6}$$

is the probability for finding an ion in a pair, and T_{eff} a fitting parameter describing the width of the steps.

C. Spin-flip Raman scattering

At low T, the Zeeman energy E_0, obtained from spin-flip light scattering from donor electrons, is given by

$$E_0 = x(\alpha N_0)\,|\,\langle S_z\rangle\,| + g^*\mu_B B \ , \tag{7}$$

when B is larger than a few tesla (where bound magnetic polaron fluctuations[17–19] can be ignored). The second term is the Zeeman splitting for g^*, the g factor in the absence of the exchange interaction. The first term of Eq. (7) is dominant and represents the *s-d* exchange between the donor electron and the Mn^{2+} ions spins, where (αN_0) is the exchange energy. Thus, the Stokes shift E_0 is nearly proportional to $|\,\langle S_z\rangle\,|$, and hence to the magnetization M. Steps in the magnetization are therefore also observed in E_0. This is the principle behind the present method to determine J_{NN}. The spin-flip energy, ignoring the small Zeeman term $g^*\mu_B B$, can be expressed in a similar manner to Eq. (5),

$$E_0 = E_s\mathcal{B}_{5/2}(y) + \delta E \sum_n \left[1+\exp\left[\frac{g\mu_B}{k_B T_{\text{eff}}}(B_n - B)\right]\right]^{-1} . \tag{8}$$

The expression for the magnetization M is similar to Eq. (8), with $\delta E/E_s = \delta M/M_s$, and δM and M_s defined in a similar manner.

D. Distant-neighbor interactions

A more refined model for the magnetization steps, which includes the effects of effective fields due to distant-neighbor exchange interactions, has been developed by Larsen *et al.*[6] This model introduces a shift, Δ, in the magnetic-field positions of *all* the steps

$$B_n = \frac{2n\,|\,J_{\text{NN}}\,|}{g\mu_B} + \Delta \ , \tag{9}$$

where Δ is the average field "felt" by the pair due to all other distant neighbor spins. Since the majority of these distant spins are singlets, which saturate below the first step, Δ has been taken to be the same for all five steps. (Strictly, Δ should increase slightly with n due to distant clusters, but this increase is small for small x.) To obtain an accurate value for the ion-ion exchange constant J_{NN}, the *difference* between the field positions of two successive steps should be measured, e.g.,

$$g\mu_B(B_2 - B_1) = 2\,|\,J_{\text{NN}}\,| \ . \tag{10}$$

We will use this formula to determine J_{NN} when the first two steps are observed. This is an improvement over the early procedure[1] in which J_{NN} was determined from B_1 using Eq. (4).

Once $|\,J_{\text{NN}}\,|$ has been determined via Eq. (10), Δ can be obtained from Eq. (9). This procedure is used when at least two steps are observed. When only a single step is observed, Δ can be *estimated* from the parameter T_0 of the Brillouin function of Eq. (5) using the relation[10]

$$\Delta \cong \frac{2k_B T_0}{(S+1)g\mu_B} . \tag{11}$$

The distant-neighbor interactions are responsible for both the shift Δ and the effective temperature T_0. In addition, these interactions broaden the steps, and are therefore responsible for the difference between T_{eff} in Eq. (5) and the actual temperature T.

III. EXPERIMENTAL TECHNIQUES

A. Spin-flip Raman scattering

Spin-flip Raman scattering measurements were carried out with the samples mounted in a fiber-optic apparatus described in Ref. 13. This probe was inserted in a cryostat which was placed in the 30-T hybrid magnet (superconductor plus Bitter solenoid). The (Cd,Mn)Se sample was immersed in ^{3}He and cooled to $T=0.5$ K, while the (Cd,Mn)Te was immersed in ^{4}He and cooled to $T=1.3$ K. The laser power incident on the sample was kept below 150 μW to avoid heating. (At powers above approximately 0.5 mW we observed a decrease in E_0, indicating heating of the Mn^{2+} spins above 0.5 K.) A Kr-ion laser operating at 1832 meV was chosen for (Cd,Mn)Se and a dye laser with LDS700 dye was chosen for the telluride sample. Polarization selection rules for spin-flip Raman scattering in (Cd,Mn)Se in a magnetic field[18] required us to align the c axis perpendicular to the field.

B. Magnetometer

Magnetization measurements were carried out using a vibrating sample magnetometer (Foner magnetometer), adapted for use in Bitter magnets which produced a maximum field of about 23 T. This instrument is superior to the very-low-frequency vibrating sample magnetometer which had been used in the early works on the magnetization steps,[1,3] because it yields a continuous trace of M versus H instead of point-by-point data. As a result, the location of the first step in the $Cd_{1-x}Mn_xSe$ sample could be located more accurately. The new instrument also has some advantages over the force magnetometer which was used in our more recent work[11] on the magnetization steps: (1) it eliminates a small spurious background and (2) the signal is strictly proportional to M, and is easily normalized to yield the absolute magnitude of M. As a result, accurate values of M_s and T_0 can be obtained from the data analysis. The force magnetometer, however, is more readily adapted for work in temperatures below 1 K.

C. Samples

The $Cd_{1-x}Mn_xSe$ sample used in the magnetization measurements was grown by the Bridgman method at Brown University. Samples from the same boule (No. I-17) were used in some of our earlier works.[1,19] The Mn concentration, determined by atomic absorption, was $x=0.049$.

The $Cd_{1-x}Mn_xTe$ sample used in the magnetization measurements was from the same Bridgman-grown boule as the sample used in the Raman measurements. The Mn concentrations in the two samples, however, were slightly different: $x=0.0325$ for the magnetization sample, and $x=0.0308$ for the Raman sample. These values are from atomic absorption. The small difference in the values of x was confirmed by magnetization measurements in a SQUID magnetometer at $T=4.2$ K and $B=5$ T.

IV. RESULTS AND DISCUSSION

A. $Cd_{0.95}Mn_{0.05}Se$

1. Spin-flip Raman scattering

Figure 1 shows a spin-flip spectrum for $Cd_{0.95}Mn_{0.05}Se$ at $B=30$ T and $T=0.5$ K. The solid line represents a fit of the data using the Gaussian form

$$F(E) \propto \exp\{[(E-E_L)-E_0]^2/2\Gamma^2\} . \tag{12}$$

Here, $F(E)$ is the scattered intensity at a Stokes energy E, E_L is the laser photon energy, E_0 is the Stokes shift of the peak, and Γ the broadening. The fit yielded E_0 to an accuracy of about 0.1 meV, which is about one-tenth of the full width at half maximum.

Figure 2 shows E_0 as a function of B to 30 T. The first two steps are clearly observed. The positions of the steps were determined with two different procedures. In the first, the low-field data (excluding the steps) between $B=3$ and 9 T were fit to the Brillouin function of Eq. (8), giving $E_s=18.4$ meV. This part was then subtracted from the high-field data. The result was then fit to the steps alone, the second term of Eq. (8), to determine B_1 and B_2. In the second method, the numerical derivative, dE_0/dB, was obtained from the raw data and the peaks in the derivative were identified as the step positions. The two methods agreed to within 2% and gave the values, $B_1=12.5\pm0.2$ T and $B_2=23.7\pm0.2$ T. We then determine $J_{NN}/k_B=-7.5\pm0.3$ K using Eq. (10). This value agrees with previous magnetization measurements in pulsed fields.[6] Table I summarizes the present results. We note that the shift in the positions of the steps

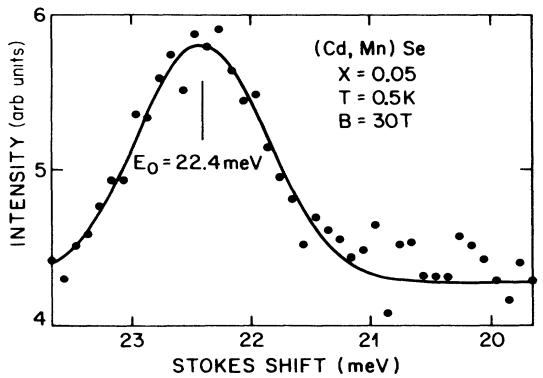

FIG. 1. Spin-flip Raman spectrum from $Cd_{1-x}Mn_xSe$, $x=0.05$, at temperature $T=0.5$ K and magnetic field $B=30$ T. The laser energy was 1832 meV. The solid line is a fit to the Gaussian form of Eq. (12), with the Zeeman energy $E_0=22.4$ meV.

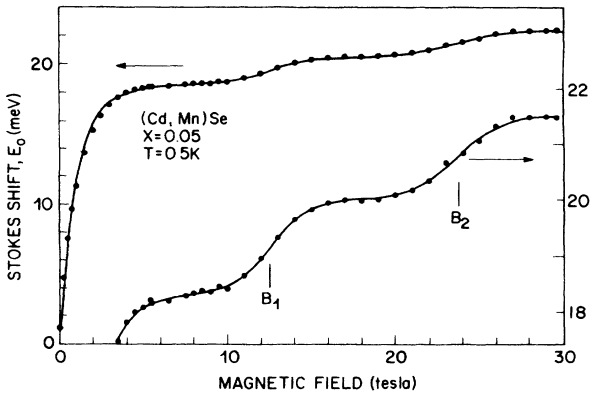

FIG. 2. Stokes shift (Zeeman energy) E_0 vs applied magnetic field B for $Cd_{1-x}Mn_xSe$, $x=0.05$, at temperature $T=0.5$ K from spin-flip Raman scattering. B_1 and B_2 denote the positions of the first and second magnetization steps of nearest-neighbor Mn-Mn pairs. The upper curve is a guide to the eye. The lower solid line is a fit to Eq. (8), with subtraction of $g^*\mu_B B$ with $g^*=+0.54$.

amounts to the difference, $\Delta=2B_1-B_2=1.3\pm.05$ T. If we apply Eq. (11) with $T_0=1.6$ determined from magnetization or Ref. 19 we get the estimate $\Delta=0.73$ T, which is lower than the result obtained from B_1 and B_2.

The relative magnitudes of the steps were determined by comparing the absolute step size, δE, to the saturating part E_s. The ratio for the first step is $\delta E/E_s=0.091$, while for the second step is $\delta E/E_s=0.083$. Assuming a random Mn distribution, the predicted value is[1,3]

$$\delta E/dE_s=(P_2/5)(x/\bar{x})=0.076\ , \tag{13}$$

in reasonable agreement with the measured results for both steps.

The dependence of the spin-flip linewidth on magnetic field is plotted in Fig. 3. Initially, the linewidth narrows with increasing magnetic field to $B=1.5$ T. This corresponds to a reduction in the magnetic fluctuations (see Refs. 16 and 18). These fluctuations are governed by the differential susceptibility dM/dB, which becomes smaller as the Mn^{2+} spins are aligned in the field. In the field range between 1.5–5 T an increase of the linewidth is observed due to compositional fluctuations. These fluctuations result from variations in the number of magnetic ions within each donor orbit, and hence to variations in the magnetic energy associated with each complex. The broadening due to compositional fluctuations is proportional to the magnetization.[20] For magnetic field $B>15$ T, the linewidth increases gradually, corresponding to the gradual increase of the magnetization due to the steps.

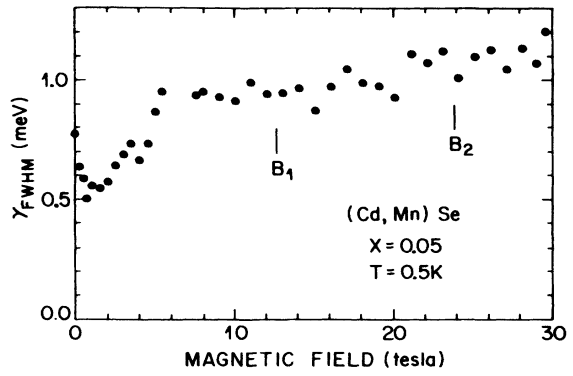

FIG. 3. Linewidth (full width at half maximum) γ vs applied magnetic field B of the spin-flip Raman spectra of $Cd_{1-x}Mn_xSe$, $x=0.05$, at temperature $T=0.5$ K. The linewidth was extracted from curve fits of the data to Eq. (12). B_1 and B_2 denote the first and second magnetic-ion-pair steps.

2. *Magnetization*

A trace of the magnetization M of $Cd_{0.951}Mn_{0.049}Se$ at 1.25 K is shown in Fig. 4. The lower curve gives an expanded view of the first step and the beginning of the second step.

The data in fields well below the first step were used to obtain the parameters M_s and T_0 of the equation

$$M=M_s\mathcal{B}_{5/2}\left[\frac{5\mu_B B}{k_B(T+T_0)}\right] \tag{14}$$

as follows. First, the background $\chi_d B$ due to the diamagnetic susceptibility of the lattice was subtracted, using the value $\chi_d=-3.3\times10^{-7}$ emu/g for CdSe.[21,22] Next, the magnetization in fields below 8 T were fit to obtain $M_s=4.51$ emu/g, $T_0=1.58$ K, and $\bar{x}=0.0305$. (These results are not sensitive to the choice of the maximum field in the fit. Changing this maximum field to 6, 7, or 9 T leads to a change of less than 0.5% in M_s, and less than 2% in T_0.) The experimental result for M_s is close to the theoretical value $M_s=4.35$ emu/g, calculated using the atomic-absorption result for x, and probabilities predict-

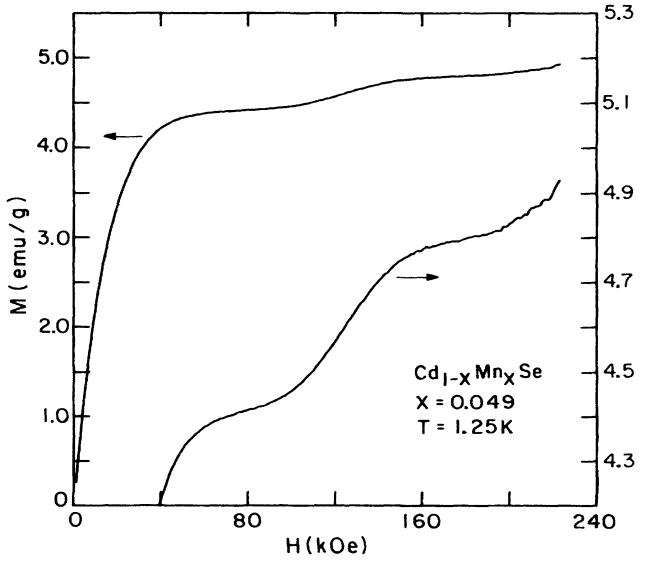

FIG. 4. Magnetization vs applied field H for $Cd_{1-x}Mn_xSe$, $x=0.049$, at temperature $T=1.25$ K.

ed for a random distribution of Mn over the cation sites.[1,3]

The data for the second step in Fig. 4 are insufficient for a reliable determination of B_2. Thus, only the field B_1 at the center of the first step was obtained. Two methods were used for this purpose. They are completely analogous to those used with SFRS data, as described previously. From the peak in the derivative dM/dH we obtained $B_1=12.5\pm0.4$ T. A fit to the second term of Eq. (8) gave $B_1=12.7$ T. The same fit also gave $\delta M/M_s=0.081$, and $T_{\rm eff}=1.53$ K. The result for $\delta M/M_s$ is close to the theoretical value $\delta M/M_s=0.079$ calculated from P_2 and $\bar{x}$ by assuming a random Mn distribution.[3] Since the value for $T_{\rm eff}$ is only 22% higher than the actual temperature T, we conclude that most of the broadening of the first step was thermal.

The magnetization results for B_1 are in good agreement with the Raman data (see Table I), and also with our earlier magnetization data. Using the magnetization value for T_0, Eqs. (9) and (11) give $J_{\rm NN}/k_B=-8.0$ K. We expect that this value is accurate to about 5%. The Raman result $J_{\rm NN}/k_B=-7.5\pm0.3$ K (which is based directly on B_2 and B_1, and thus avoids the estimate of Δ) is consistent with this conclusion. It is noteworthy that the value $J_{\rm NN}/k_B=-8.3$ K quoted in Ref. 1 was based on a simplified model which ignored the correction Δ.

B. $Cd_{0.97}Mn_{0.03}Te$

1. *Spin-flip Raman scattering*

The steps in the telluride are less clear than in the selenide sample because: (1) the g value for CdTe is negative ($g^*=-0.8$), which produces a background with a negative slope at high fields and (2) the first step is somewhat obscured by the "knee" in the Brillouin part of the magnetization. Nevertheless, a simple subtraction of the Zeeman term reveals the first three steps. The lower curve and set of data in Fig. 5 show the steps in $Cd_{0.97}Mn_{0.03}Te$ to 30 T at $T=1.3$ K, after this subtraction. The positions of the steps were determined in the same fashion as for the selenide-based material by first subtracting the saturating part using $E_s=11.45$ meV and the magnetization value $T_0=1.5$ K. We then determined the field positions of the steps to be, $B_1=10.0\pm1$ T, $B_2=18.9\pm0.2$ T, and $B_3=29\pm1$ T. The large error bar

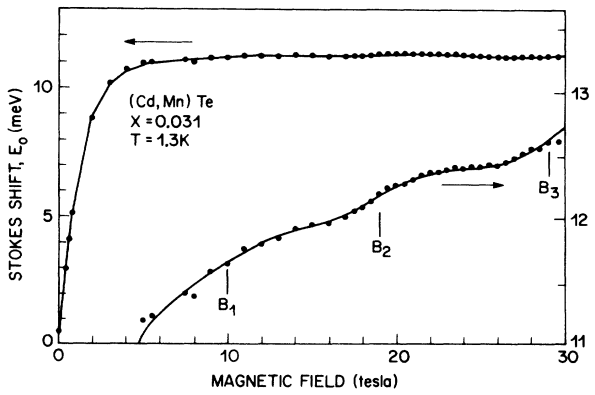

FIG. 5. Stokes shift (Zeeman energy) E_0 vs applied magnetic field B for $Cd_{1-x}Mn_xTe$, $x=0.03$, at temperature $T=1.3$ K. The upper curve is a guide to the eye. The lower data and the fit to Eq. (8) (solid line) have the background $g^*\mu_B B$, with $g^*=-0.8$, subtracted. B_1, B_2, and B_3 denote the pair steps.

for B_1 is due to the incomplete saturation of the Brillouin function. The highest portion of the third step could not be reached with the available field. To obtain $J_{\rm NN}$, we only use the first two steps. This gives $J_{\rm NN}=-6.0\pm1$ K, in reasonable agreement with the magnetization data and previous determinations.[11]

Using Eq. (11) with the value $T_0=1.5$ K obtained below, we get $\Delta=0.64$ T. This gives $J_{\rm NN}/k_B=-6.3$ K from the first step and $J_{\rm NN}/k_B=-6.1$ K from the second, which are both improvements over the value of $J_{\rm NN}/k_B=-6.7$ K, predicted from the position of the first step with no Δ correction. Since the position of the second step is most accurately determined, the value $J_{\rm NN}/k_B=-6.1\pm0.2$ K obtained from it, using Eqs. (9) and (11), is the most reliable. The uncertainty of 0.2 K in this value is partially due to the uncertainty in Δ.

The relative magnitudes of the steps are $\delta E_1/E_s=0.044$, $\delta E_2/E_s=0.037$, and $\delta E_3/E_s=0.039$. The predicted step size for an $x=0.030$ sample is 0.056. This discrepancy is probably due to inaccurate subtraction of the Zeeman term $g^*\mu_B B$.

2. *Magnetization*

A trace of the magnetization of $Cd_{1-x}Mn_xTe$ at 1.28 K is shown in Fig. 6. The lower curve gives an expanded

TABLE I. Parameters determined from steps in the magnetization (MAG) and spin-flip Raman scattering (SFRS) experiments. The values for T_0 were obtained by fitting $M(B)$ to the Brillouin function of Eq. (14). B_1, B_2, and B_3 are the field values of the first three steps, and $J_{\rm NN}$ is the nearest-neighbor Mn-Mn exchange energy derived from the steps as discussed in the text.

Material	Experiment	T_0 (K)	B_1 (T)	B_2 (T)	B_3 (T)	$-J_{\rm NN}/k_B$ (K)
$Cd_{1-x}Mn_xSe$	SFRS		12.5±0.2	23.7±0.2		7.5±0.3
$x=0.049$	MAG	1.58	12.5±0.4			8.0±0.5
$Cd_{1-x}Mn_xTe$	SFRS		10.1±1	18.9±0.2	29±1	6.1±0.2
$x=0.03$	MAG	1.53	10.2±0.3	18.9±0.3		6.1±0.3

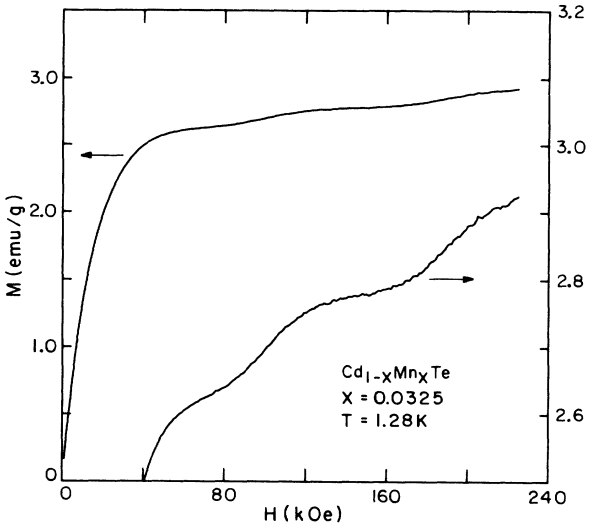

FIG. 6. Magnetization vs applied field H for $Cd_{1-x}Mn_xTe$, $x=0.033$, at temperature $T=1.28$ K.

view of the first two steps. The analysis of the data for fields well below the first step was similar to that for (Cd,Mn)Se. The diamagnetic contribution of the lattice was subtracted using $\chi_d=-3.5\times10^{-7}$ emu/g (Ref. 21). A fit of the data below 5.0 T to Eq. (14) then gave $M_s=2.68$ emu/g and $T_0=1.53$ K. (Fits for data below 4 or 6 T gave practically the same results.) The result for M_s is in excellent agreement with the theoretical value $M_s=2.67$ emu/g, based on the atomic-absorption value for x and the assumption of a random Mn distribution.

The values of B_1 and B_2 at the centers of the first two steps were obtained from the peaks in dM/dH. [As discussed in Ref. 11, this method is preferable in this case to that based on fits to Eq. (8).] The results were $B_1=10.2\pm0.3$ T and $B_2=18.95\pm0.3$ T. These are in agreement with the Raman data. From the difference (B_2-B_1) and Eq. (10) we obtain $J_{NN}/k_B=-5.9\pm0.3$ K. Using Eq. (11) for Δ, in conjunction with the magnetization value for T_0, the result for B_1 and Eq. (9) gives $J_{NN}/k_B=-6.4$ K. The same procedure applied to B_2 gives $J_{NN}/k_B=-6.1$ K. We regard the latter value as more reliable because the percentage contribution of the correction Δ to the right-hand-side of Eq. (9) is proportional to $1/n$. These results for J_{NN} are in good agreement both with the Raman determination of J_{NN} and with the earlier result $J_{NN}/k_B=-6.1\pm0.3$ K from the magnetization steps on a sample with $x=0.047$.[11]

3. *Comparison of SFRS and Magnetization*

Finally, we determine a value for the s-d exchange constant αN_0 by comparing the spin-flip Raman scattering data with magnetization data. Combining Eqs. (1), (7) and (8), we get

$$\alpha N_0=\frac{2\mu_B A}{W}\frac{E_s}{M_s} . \tag{15}$$

Since the samples used in SFRS and magnetization had slightly different x, we adjusted the value of M_s. This gave $M_s=2.54$ emu/g for the Raman sample. Thus,

$$(\alpha N_0)=211\pm10 \text{ meV} .$$

(Cd,Mn)Te with this method and agrees with the band-edge, free-exciton magnetoreflectance value $\alpha N_0=220$ meV (Ref. 23).

V. SUMMARY

For increasing magnetic field, we observe transitions of the magnetic-ion-pair from the spin $S_T=0$ ground state to the $S_T=1$, $S_T=2$, and $S_T=3$ excited states. The fields at which these transitions or steps occur correspond to the points at which the energy of the higher-lying state falls below that for the next-lower state. For truly isolated pairs the field positions should occur at integer multiples of the field of the first step. However, since many of the pairs will have an ion at a next-nearest-neighbor site, all the steps are biased to higher fields by an effective field due to the further neighbors. The optical data support this notion—the separation between the first and second steps is smaller than the field of the first step. Table I summarizes these results. Thus, more accurate results are obtained for J_{NN} by taking the *difference between steps*. This method produced $J_{NN}/k_B=-7.5$ K for (Cd,Mn)Se. On the other hand, if the first step is not well defined (due to nonsaturation of the Brillouin function), J_{NN} is best determined from *the second step and the* Δ *correction*. This was used to obtain $J_{NN}/k_B=-6.1$ K for (Cd,Mn)Te. The values of Δ estimated from T_0 are smaller than those deduced from B_n by about a factor of 2. Thus, this method of determining J_{NN} using Δ should be treated as only a first-order correction.

In principle, both optical and magnetic techniques are equally valid for studying the steps. Differences are therefore largely due to the present states of the art for both techniques. At present, the magnetization method has the advantage of: (1) a somewhat better signal-to-noise ratio in high fields and (2) a continuous trace versus point-by-point data. These advantages are offset by the higher fields which presently can be used with the fiber-optics Raman spectrometer. This higher-field advantage is particularly significant when it leads to the observation of the second step, as in the case of (Cd,Mn)Se, because J_{NN} is more accurately determined from B_2-B_1 than from B_1 and the estimated correction Δ.

ACKNOWLEDGMENTS

This work is supported by the National Science Foundation Grant Nos. DMR-8504366 and DMR-8601345, and U.S. Defense Advanced Research Projects Agency (Sunnyvale, CA), Contract No. N00014-86-0760. The Francis Bitter National Magnet Laboratory is supported by the National Science Foundation under cooperative agreement Grant No. DMR-8511789. E. D. Isaacs received support from AT&T.

*Also Department of Physics. Present address: AT&T Bell Laboratory, Murray Hill, NJ 07974.

[1]Y. Shapira, S. Foner, D. H. Ridgley, K. Dwight, and A. Wold, Phys. Rev. B **30**, 4021 (1984).

[2]R. L. Aggarwal, S. N. Jasperson, Y. Shapira, S. Foner, T. Sakakibara, T. Goto, N. Miura, K. Dwight, and A. Wold, in *Proceedings of the 17th International Conference on the Physics of Semiconductors, San Francisco, 1984,* edited by J. D. Chadi and W. A. Harrison (Springer-Verlag, New York, 1985), p. 1419.

[3]Y. Shapira, S. Foner, P. Becla, D. N. Domingues, M. J. Naughton, and J. S. Brooks, Phys. Rev. B **33**, 356 (1986).

[4]R. L. Aggarwal, S. N. Jasperson, P. Becla, and J. K. Furdyna, Phys. Rev. B **34**, 5894 (1986).

[5]R. L. Aggarwal, S. N. Jasperson, P. Becla, and R. R. Galazka, Phys. Rev. B **32**, 5132 (1985).

[6]B. E. Larson, K. C. Hass, and R. L. Aggarwal, Phys. Rev. B **33**, 1789 (1986).

[7]N. Yamada, S. Takeyama, T. Sakakibara, T. Goto, and N. Miura, Phys. Rev. B **34**, 4121 (1986).

[8]D. Heiman, P. Becla, R. B. Kershaw, D. Ridgley, K. Dwight, A. Wold, and R. R. Galazka, Phys. Rev. B **34**, 3961 (1986).

[9]M. Gorska and J. R. Anderson, in Proceedings of the International Meeting on the Physics of Semimagnetic Semiconductors, 1987, Jablonna, Poland (unpublished).

[10]G. Barilero, C. Rigaux, Hguyen Hy Hau, J. C. Picoche, and W. Giriat, Solid State Commun. **62**, 345 (1987).

[11]Y. Shapria and N. F. Oliveira, Jr., Phys. Rev. B **35**, 6888 (1987).

[12]D. Heiman (unpublished).

[13]E. D. Isaacs and D. Heiman, Rev. Sci. Instrum. **58**, 1672 (1987).

[14]S. Nagata, R. R. Galazka, D. P. Mullin, H. Akbarzadeh, G. D. Khattak, J. K. Furdyna, and P. H. Keesom, Phys. Rev. B **22**, 3331 (1980).

[15]M. M. Kreitman, F. J. Milford, R. P. Kenan, and J. G. Daunt, Phys. Rev. **144**, 367 (1966).

[16]E. D. Isaacs, D. Heiman, M. J. Graf, B. B. Goldberg, R. Kershaw, D. Ridgley, K. Dwight, A. Wold, J. K. Furdyna, and J. S. Brooks, Phys. Rev. B **37**, 7108 (1988).

[17]T. Dietl and J. Spalek, Phys. Rev. B **28**, 1548 (1983); Phys. Rev. Lett. **48**, 355 (1982).

[18]D. Heiman, P. A. Wolff, and J. Warnock, Phys. Rev. B **27**, 4848 (1983).

[19]D. Heiman, Y. Shapira, S. Foner, B. Khazai, R. Kershaw, K. Dwight, and A. Wold, Phys. Rev. B **29**, 5634 (1984).

[20]D. Heiman, A. Petrou, S. Bloom, Y. Shapira, E. D. Isaacs, and W. Giriat, Phys. Rev. Lett. **60**, 1876 (1988).

[21]M. E. Lines and J. V. Waszczak, J. Appl. Phys. **48**, 1395 (1977); V. I. Ivanov-Omskii, B. T. Kolomiets, V. M. Mel'nik, and V. K. Ogorodnikov, Fiz. Tverd. Tela (Leningrad) **11**, 2563 (1969) [Sov. Phys.—Solid State **11**, 2067 (1970)].

[22]Y. Shapira (unpublished).

[23]J. A. Gaj, R. Planel, and G. Fishman, Solid State Commun. **29**, 435 (1979).